

Incorporation of Piperazino Functionality into 1,3-Disubstituted Urea as the Tertiary Pharmacophore Affording Potent Inhibitors of Soluble Epoxide Hydrolase with Improved Pharmacokinetic Properties

Shao-Xu Huang,[†] Hui-Yuan Li,[†] Jun-Yan Liu,[‡] Christophe Morisseau,[‡] Bruce D. Hammock,[‡] and Ya-Qiu Long^{*,†}

[†]State Key Laboratory of Drug Research, Shanghai Institute of Materia Medica, Chinese Academy of Sciences, 555 Zuchongzhi Road, Shanghai 201203, China, and [‡]Department of Entomology and University of California Davis Cancer Center, University of California, One Shields Avenue, Davis, California 95616, United States

Received August 23, 2010

The inhibition of the mammalian soluble epoxide hydrolase (sEH) is a promising new therapy in the treatment of hypertension, inflammation, and other disorders. However, the problems of limited water solubility, high melting point, and low metabolic stability complicated the development of 1,3-disubstituted urea-based sEH inhibitors. The current study explored the introduction of the substituted piperazino group as the tertiary pharmacophore, which resulted in substantial improvements in pharmacokinetic parameters over previously reported 1-adamantylurea based inhibitors while retaining high potency. The SAR studies revealed that the meta- or para-substituted phenyl spacer and *N*⁴-acetyl or sulfonyl substituted piperazine were optimal structures for achieving high potency and good physical properties. The 1-(4-(4-(4-acetylpiperazin-1-yl)butoxy)phenyl)-3-adamantan-1-yl urea (**29c**) demonstrated excellent in vivo pharmacokinetic properties in mice: $T_{1/2} = 14$ h, $C_{max} = 84$ nM, $AUC = 40\,200$ nM·min, and $IC_{50} = 7.0$ nM against human sEH enzyme.

Introduction

Epoxide hydrolases (EHs, E.C.3.3.2.3) are a group of ubiquitous enzymes present in most living organisms. They catalyze the addition of water to an epoxide, resulting in the formation of a vicinal diol.¹ In mammals, several types of EHs have been identified including leukotriene A₄ hydrolase, cholesterol epoxide hydrolase,² hepxoxilin hydrolase,³ microsomal epoxide hydrolase (mEH), and soluble epoxide hydrolase (sEH^a),⁴ which differ in their substrate specificity. The first three enzymes are not α/β fold family, while the last two are. Among the α/β fold family, the sEH is of particular therapeutic interest because of its involvement in the metabolism of endogenously derived fatty acid epoxides and other lipid epoxides.⁵

The sEH promotes the hydrolysis of the biologically active epoxyeicosatrienoic acids (EETs) to the pharmacologically less active and more rapidly cleared dihydroxyepoxyeicosatrienoic acids (DHETs).^{4,6} As the primary metabolites of cytochrome P450 epoxygenases of arachidonic acid,⁷ EETs are known to regulate blood pressure and inflammation.^{8,9} In addition, the EETs have vascular protective effects such as suppression of reactive oxygen species following hypoxia–reoxygenation,¹⁰ attenuation of vascular smooth muscle

migration,¹¹ and enhancement of a fibrinolytic pathway.¹² However, the metabolism of EETs to DHETs by sEH often leads to reductions in these biological activities.¹³ Thus, stabilizing the in vivo concentration of EETs through pharmacological intervention by sEH inhibitors is a novel and potentially therapeutic avenue to treat hypertension, inflammation, and other cardiovascular disorders.¹⁴ It has been reported that sEH inhibitors significantly reduce blood pressure of most varieties of the spontaneous hypertensive rats and angiotensin II induced hypertensive rats.^{5,15–18} As such, an sEH inhibitor, AR9281, currently began clinical phase IIa trial for the treatment of type 2 diabetes mellitus and hypertension,¹⁹ which has in turn fueled the recent surge of interest in the development of sEH inhibitors.^{20–27}

To date, the most successful sEH inhibitors are 1,3-disubstituted ureas, which display antihypertension and anti-inflammatory effects through inhibition of EET hydrolysis in several cellular and animal models.^{5,17} Common structural features of these inhibitors are the large hydrophobic domains flanking their central urea pharmacophore, which is believed to engage in the hydrogen bond formation with the active site residues Tyr381, Tyr465, and Asp333 of sEH enzyme.⁴ However, the urea-based inhibitors often suffer from poor solubility and bioavailability, which hinders their pharmacological use in vivo. During efforts to improve the potency and physicochemical properties, a new concept of a secondary pharmacophore was proposed, referring to a polar functional group located on the fifth/sixth atom (7.5 Å) from the carbonyl group of the urea primary pharmacophore to help improve the binding and the water solubility (Figure 1).^{28,29} In addition, there also existed a tertiary pharmacophore that is located on the 14th to 16th atom (~17 Å) from the carbonyl group of the urea primary pharmacophore (Figure 1). An acidic or

*To whom correspondence should be addressed. Phone: 86-21-50806876. Fax: +86-21-50806876. E-mail: yqlong@mail.shnc.ac.cn.

^a Abbreviations: sEH, soluble epoxide hydrolase; EET, epoxyeicosatrienoic acid; DHET, dihydroxyepoxyeicosatrienoic acid; AEP, 1-adamantan-1-yl-3-[5-[2-(2-ethoxyethoxy)ethoxy]pentyl]urea; t-AUCB, *trans*-4-[4-(3-adamantan-1-ylureido)cyclohexyloxy]benzoic acid; AUDA, 12-(3-adamantan-1-ylureido)dodecanoic acid; APAU, *N*-(1-acetylpiperidin-4-yl)-*N'*-(adamant-1-yl)urea; AMCU, 1-adamantan-1-yl-3-(4-(3-morpholinopropoxy)cyclohexyl)urea; $T_{1/2}$, half-life; C_{max} , maximum concentration; IC_{50} , half maximal inhibitory concentration; AUC_t , area under the concentration–time curve to terminal time.

ester group as the tertiary pharmacophore or a polar group such as ester, sulfonamide, ketone, alcohol, or ether as the secondary pharmacophore was effective for producing soluble inhibitors in either water or oil while retaining inhibitory potency (Figure 2). However, relatively short half-lives and in some cases poor bioavailability were still observed with these inhibitors.^{30,31}

In order to improve the physical and pharmacokinetic properties of these urea-based sEH inhibitors while retaining potency, we were intrigued to incorporate a constrained heterocycle as a polar functionality on the 1,3-dialkylurea platform. Piperazine is an interesting heterocycle structure present in many biologically active molecules, conferring metabolic stability and potentiating interactions with macromolecules.^{32,33} We have tried a substituted piperazino group as the secondary pharmacophore on the 1-adamantylurea scaffold.³⁴ As expected, these piperazino-containing sEH inhibitors displayed excellent water solubility and low melting point, but their inhibitory activity was remarkably decreased. Since the piperazino functionality is beneficial for the physical properties, we decided to try the piperazino group as the tertiary pharmacophore in the urea-based sEH inhibitors to gain an improvement in the solubility and bioavailability without any loss of inhibitory activity. Combining the favorable structures obtained from the previous SAR studies, we designed a new class of 1,3-disubstituted ureas functionalized with piperazino group on the tertiary pharmacophore while retaining ether as the secondary pharmacophore and choosing the phenyl ring and the alkyl chain as the linkers between the primary and secondary and tertiary pharmacophores, respectively (Figure 2). In this study, the substituted piperazino pharmacophore, the orientation of the phenyl spacer, and the length of the alkyl chain were investigated with respect to the

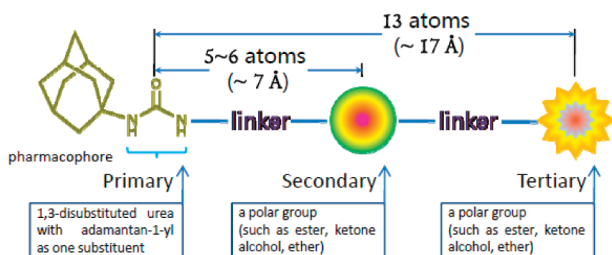


Figure 1. Proposed pharmacophore model for urea-based sEH inhibitors.

effect on the activity and physical and pharmacokinetic properties of the 1,3-disubstituted urea-based sEH inhibitors.

Chemistry

Scheme 1 outlines the syntheses of the 1-adamantan-1-yl 3-substituted ureas having a phenyl ring between the urea group and the piperazino group in a para-, meta-, or ortho-substitution pattern, separately. The piperazino group was located on the tertiary pharmacophore site and connected with the phenyl ring via an alkoxy linker with various chain lengths. These 1-adamantan-1-yl-3-(piperazin-1-yl)alkoxyphenylureas were synthesized by coupling 1-adamantyl isocyanate with various amines in DCM. In this article, when the piperazino ring was *N*-substituted unsymmetrically, *N*¹ represents the left-hand side nitrogen atom closer to the urea pharmacophore while *N*⁴ represents the right-hand side nitrogen atom.

The preparation of various amines was commenced with commercially available *o*-, *m*-, or *p*-nitrophenol and α,ω -dibromoalkane (i.e., 1,2-dibromoethane for compound **3b**, 1,3-dibromopropane for compounds **4a–c**, 1,4-dibromobutane for compounds **5a–c**, 1,5-dibromopentane for compound **6b**). The nucleophilic substitution followed by the alkylation with 1-methylpiperazine (for compounds **7b**, **8a–c**, **9a–c**, and **10b**) or *tert*-butyl piperazine-1-carboxylate (for compounds **11b**, **12a,b**, **13a–c**, and **14b**) gave compounds bearing a piperazino group. Sequential reduction of the nitro group and condensation with 1-adamantyl isocyanate furnished the *N,N'*-disubstituted ureas (**15–22**)a–c. Further deprotection and acetylation on the *N*⁴ atom of the piperazino ring yielded the corresponding *N*⁴-unsubstituted piperazine-containing compounds (**23–26**)a–c and the *N*⁴-acetyl protected derivatives (**27–30**)a–c, respectively.

In order to optimize the synthetic route for an extensive SAR study, we established alternative approaches to synthesize the substituted piperazine-containing ureas, as depicted in Scheme 1B and Scheme 1C. First, the piperazine unit was introduced from the reaction of 1-(ω -bromoalkoxy)-(2, 3, or 4)-nitrobenzenes (**3–6**)a–c with free piperazine. Then the *N*⁴-unsubstituted piperazino moiety was transformed into variously *N*⁴-substituted analogues in a similar manner as Scheme 1A indicated. Alternatively, the *N*⁴-Boc protected intermediates (**11–14**)a–c could be used to perform the *N*⁴-protecting group exchange prior to the coupling with the isocyanate.

On the other hand, we were interested in introducing functionality on the alkyl linker between the ether secondary

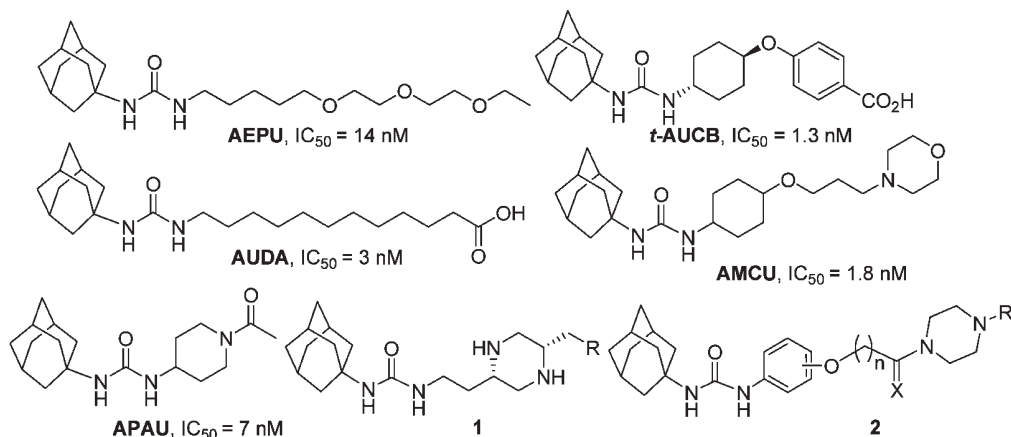
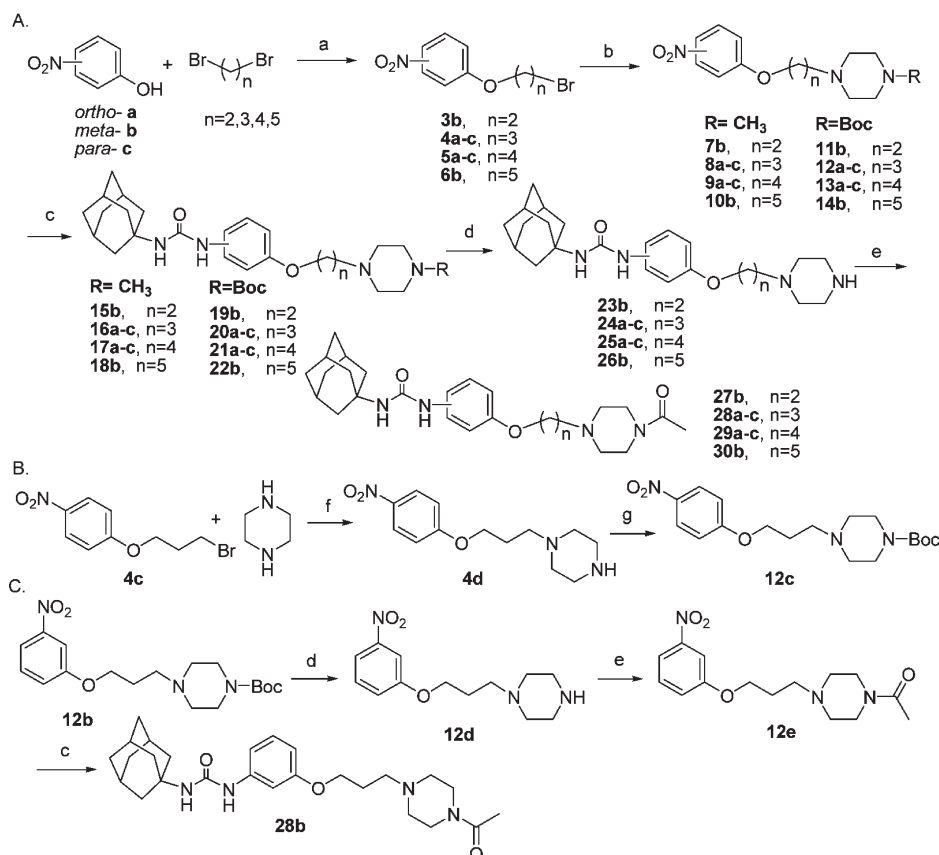
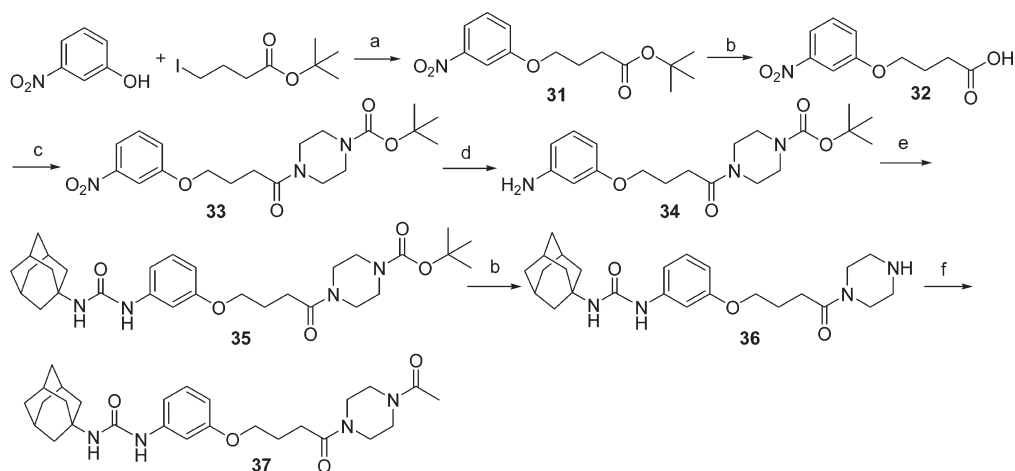


Figure 2. Representative urea-based sEH inhibitors and our designed piperazino-containing series.

Scheme 1. Synthesis of 1-Adamantan-1-ylurea Derivatives with Piperazine Group Present in the Tertiary Pharmacophore Region^a

^a Reagents and conditions: (a) K_2CO_3 , DMF, room temp; (b) 1-methylpiperazine (for compounds **7b**, **8a-c**, **9a-c**, and **10b**) or *tert*-butyl piperazine-1-carboxylate (**11b**, **12a-c**, **13a,b**, and **14b**), THF, reflux; (c) (i) H_2 (1 atm), 10% Pd/C, CH_3OH , room temp; (ii) 1-adamantyl isocyanate, DCM, 0°C to room temp; (d) TFA, DCM, 0°C to room temp; (e) Ac_2O , DCM, room temp; (f) Et_3N , DMF, reflux; (g) di-*tert*-butyl dicarbonate, CH_3OH , room temp.

Scheme 2. Synthesis of 1-Adamantan-1-yl-3-(3-(4-oxo-4-(piperazin-1-yl)butoxy)phenyl)urea Derivatives^a

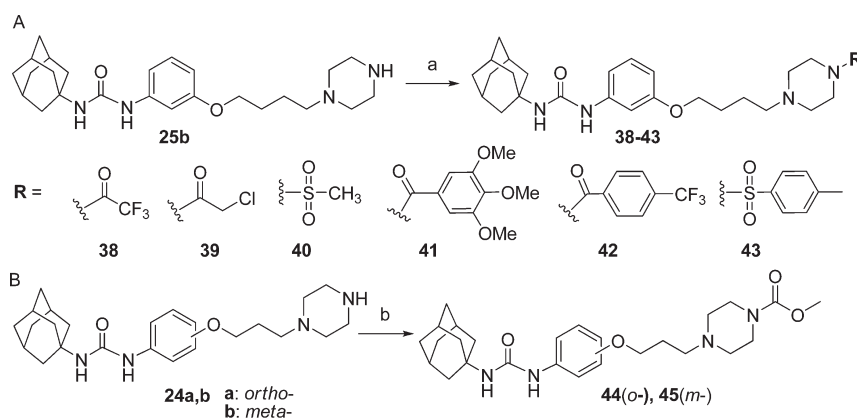
^a Reagents and conditions: (a) K_2CO_3 , DMF, room temp; (b) TFA, DCM, room temp; (c) *tert*-butyl piperazine-1-carboxylate, HOAt, EDCI, DIPEA, DCM, room temp; (d) H_2 (1 atm), 10% Pd/C, CH_3OH , room temp; (e) 1-adamantyl isocyanate, DCM, 0°C to room temp; (f) Ac_2O , DCM, room temp.

pharmacophore and the piperazine tertiary pharmacophore. Scheme 2 describes the synthesis of such an analogue bearing a carbonyl group on the *N*¹-piperazine. Reaction of *m*-nitrophenol with *tert*-butyl 4-iodobutanoate generated the precursor *tert*-butyl 4-(3-nitrophenoxy)butanoate **31**. The subsequent deprotection of the carboxyl group followed by the amidation with *tert*-butyl piperazine-1-carboxylate in the presence of

HOAt and EDCI gave the *tert*-butyl 4-(4-(3-nitrophenoxy)-butanoyl)piperazine-1-carboxylate (**33**). Then a similar strategy as Scheme 1 indicated was employed, affording the target compound **1**-3-(4-(4-(4-acetylpiperazin-1-yl)-4-oxobutoxy)phenyl)-3-adamantan-1-ylurea (**37**).

The substitution effect on *N*⁴-piperazine of the urea inhibitors was investigated. The preparation of various *N*⁴-substituted

Scheme 3. Synthesis of 1-Adamantan-1-yl-3-(3-(4-(piperazin-1-yl)butoxy)phenyl)urea Derivatives with Different N^4 -Substituents on Piperazine Ring (A) and 1-Adamantan-1-yl-3-(3(or 2)-(3-(piperazin-1-yl)propoxy)phenyl)urea Derivatives with N^4 -Methoxycarbonyl (B)^a



^a Reagents and conditions: (a) trifluoroacetic anhydride, Et₃N, DCM, room temp for compound **38**; 2-chloroacetyl chloride, Et₃N, DCM, room temp for compound **39**; methanesulfonyl chloride, Et₃N, DCM, room temp for compound **40**; 3,4,5-trimethoxybenzoic acid, HOAt, EDCI, DIPEA, DCM, room temp for compound **41**; 4-(trifluoromethyl)benzoic acid, HOAt, EDCI, DIPEA, DCM, room temp for compound **42**; 4-methylbenzene-1-sulfonyl chloride, Et₃N, DCM, room temp for compound **43**; (b) methyl carbonochloridate, Et₃N, DCM, room temp.

piperazine-containing 1-adamantan-1-yl-3-substituted ureas is depicted in Scheme 3. Starting from 1-adamantan-1-yl-3-(3-(4-(piperazin-1-yl)butoxy)phenyl)urea (**25b**), reaction with various acylating agents furnished the target products **38–43** in 50–88% yield.

Results and Discussion

To obtain potent sEH inhibitors with improved physical and pharmacokinetic properties, a variety of 1,3-disubstituted ureas functionalized with piperazine as the tertiary pharmacophore were explored in this study. As a constrained hydrophilic heterocycle, the piperazino group has been reported to be beneficial for the water solubility and metabolic stability for many drugs.^{32,33} Our previous effort to incorporate the piperazino group into the secondary pharmacophore of the urea inhibitors dramatically improved the physical properties of the compounds at the cost of lost potency.³⁴ On the basis of the pharmacophore model, herein we incorporated the piperazino group into the tertiary pharmacophore of 1-adamantan-1-yl-3-alkoxyphenylurea platform and examined the optimal positioning and substitution of the piperazino functionality.

In the design of the scaffold, we combined the favorable structures obtained from the previous SAR studies, e.g., the ether as the secondary pharmacophore, the phenyl ring as the linker between the primary and secondary pharmacophores, the flexible carbon chain as the linker between the secondary and tertiary pharmacophores. The phenyl ring can provide ortho-, meta-, and para-substitution patterns to determine the optimal orientation of the secondary ether bearing a piperazine tail relative to the primary urea. For the linker between the piperazine and the oxygen atom in the ether group, we initially selected propyl and butyl chains to meet the distance requirement between the secondary and tertiary pharmacophore. We investigated varying carbon chain length further to determine an appropriate location for the incorporated piperazine functionality. In addition, the substituent on the N^4 -atom of the piperazine was investigated to achieve an optimal balance between the hydrophilicity and the hydrophobicity for the tertiary pharmacophore, in which N^4 - and N^1 -substitution varied in a range of acyl groups and alkyl groups.

Table 1. Inhibition of Human sEH and Melting Points of 1-Adamantan-1-yl-3-(piperazin-1-ylalkoxyphenyl)urea Derivatives with Variation on the Phenyl Substitution Position and Piperazine-4-yl Substitution

<i>n</i>	substitution mode	compd	R	mp ^a (°C)	IC ₅₀ ^b (nM)
3	ortho	24a	H	162–164	97460
		16a	CH ₃	154–156	2880
		28a	CH ₃ CO	86–88	994
	meta	24b	H	84–86	27.2
		16b	CH ₃	144–146	23.1
	para	28b	CH ₃ CO	96–98	3.6
		24c	H	104–106	156
		16c	CH ₃	98–100	17.9
4	ortho	28c	CH ₃ CO	170–172	3.3
		25a	H	147–149	72770
		17a	CH ₃	120–122	5290
	meta	29a	CH ₃ CO	98–100	3150
		25b	H	94–96	14.8
		17b	CH ₃	115–117	13.3
	para	29b	CH ₃ CO	76–78	2.7
		25c	H	87–90	126
		17c	CH ₃	118–121	44.8
		29c	CH ₃ CO	150–152	7.0

^a mp, melting point. ^b The IC₅₀ values were determined by a sensitive fluorescent assay on human sEH.³⁵

The meta- or para-substituted phenyl linker is favored for the sEH inhibition, while the ortho-substitution is detrimental. The effect of the piperazine pharmacophore on enzyme inhibition and physical properties was investigated with regard to the phenyl substitution pattern and the N^4 -piperazino substitution. The activity data of these ureas are summarized in Table 1. In general, the inhibitory activity of this series of ureas bearing piperazine as the tertiary pharmacophore was far superior to that of the analogues carrying piperazine as secondary pharmacophore reported previously.³⁴ Furthermore, the melting point was desirably low to moderate for this class. Although melting point is usually a minor consideration, high melting point and lipophilic

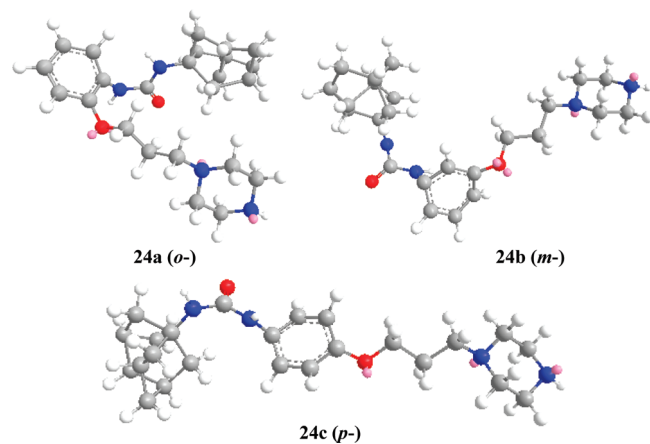


Figure 3. Possible conformations of the ortho-, meta-, and para-substituted phenyl containing ureas with minimized energy.

compounds are not soluble and hard to formulate. Usually, $\sim 70\text{ }^{\circ}\text{C}$ is high enough to crystallize if needed and not melt in tablet press. The lower the melting point, the less chance there is of polymorphs and the more easily soluble are the lipophilic compounds.

Obviously, the spacial arrangement of the primary urea and the secondary ether bearing a piperazine tail played an important role in the inhibitory potency against human sEH enzyme. As shown in Table 1, the meta-substituted ureas (e.g., **24b**, **16b**, **28b**) were remarkably more potent than the ortho-substituted counterparts (**24a**, **16a**, **28a**), whereas the para-substituted analogues (**24c**, **16c**, **28c**) were nearly as potent as the meta-substituted ones when the N^4 on the piperazine ring was substituted. As for the meta derivatives, the acetamide was more potent than the tertiary amine.

To understand the observation that the ortho-substitution caused a significant loss of the inhibitory potency on the enzyme compared to the meta- and para-substitution, we calculated the possible conformations of the three isomers (**24a–c**) by running MM2/minimize energy through Chemoffice Chem3D Ultra 9.0. As demonstrated in Figure 3, the steric hindrance conferred by the ortho-substituent on the phenyl ring might prevent the primary urea pharmacophore from interacting properly with the key residues in the binding pocket of sEH, resulting in a low potency.

Besides the substitution pattern of the phenyl spacer, the N^4 -substituent on the piperazine pharmacophore also affected the inhibitory activity dramatically. As indicated in Table 1, N^4 -acetyl substituted piperazine containing ureas (**28a–c**, **29a–c**) were much more potent than the corresponding N^4 -unsubstituted analogues (**24a–c**, **25a–c**), while the N^4 -methyl substituted piperazine containing ureas (**16a–c**, **17a–c**) were slightly less potent than the N^4 -acetyl substituted counterparts. Taking the meta-substituted phenyl bridged ureas as examples, the N^4 -acetylpiperazine containing urea (**28c**, $\text{IC}_{50} = 3.3\text{ nM}$) exhibited a 47.2- and 5.4-fold increase in the potency relative to the N^4 -unsubstituted (**24c**, $\text{IC}_{50} = 156\text{ nM}$) and N^4 -methyl substituted (**16c**, $\text{IC}_{50} = 17.9\text{ nM}$) analogues, respectively. The differentiating effect might be attributed to the presence of the hydrogen bond acceptor, i.e., carbonyl group on the piperazine and the reduction of the polarity at this site. Previous studies have demonstrated that increasing lipophilicity trended toward more potent sEH inhibitors,^{36,37} as expected from the hydrophobic catalytic site shown by crystal structures.³⁸ Therefore, reducing the polarity of the

Table 2. Inhibition of Human sEH and Melting Point of 1-Adamantan-1-yl-3-(3-(4-(piperazin-1-yl)butoxy)phenyl)urea and 1-Adamantan-1-yl-3-(3-(4-oxo-4-(piperazin-1-yl)butoxy)phenyl)urea Derivatives with N^4 -Unsubstituted or N^4 -Acetylated Piperazine

Compd.	X	R	Mp ^a ($^{\circ}\text{C}$)	IC_{50}^b (nM)
25b	H ₂	H	94–96	14.8
36	O	H	78–80	91.4
21b	H ₂		135–137	7.1
35	O		100–104	21.5
29b	H ₂		76–78	2.7
37	O		90–92	5.4

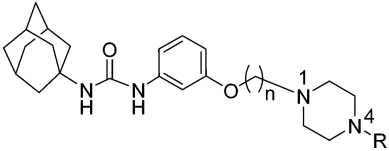
^aMp, melting point. ^bThe IC_{50} values were determined by the sensitive fluorescent assay on human sEH.³⁵

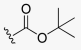
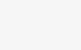
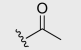
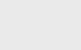
N^4 -piperazine by introducing an N^4 -substituent such as a methyl or acetyl group resulted in the increase of the potency in the context of piperazine as the tertiary pharmacophore.

Inspired by the potentiating effect of N^4 -acetyl substitution, we started to investigate the impact of the acylating the N^1 atom in the piperazine pharmacophore on the enzyme inhibition. Taking the *m*-phenoxybutyl bridged urea as a convenient platform, we employed the synthetic route as presented in Scheme 2 to obtain N^1 -acylated piperazine containing compounds and tested the enzyme IC_{50} values. However, all the N^1 -acylated compounds turned out 2.0- to 6.2-fold less potent than the corresponding N^1 -alkylated analogues with respect to the sEH inhibition regardless of the N^4 -substitution (Table 2, **36** $\text{IC}_{50} = 91.4\text{ nM}$ vs **25b** $\text{IC}_{50} = 14.8\text{ nM}$; **35** $\text{IC}_{50} = 21.5\text{ nM}$ vs **21b** $\text{IC}_{50} = 7.1\text{ nM}$; **37** $\text{IC}_{50} = 5.4\text{ nM}$ vs **29b** $\text{IC}_{50} = 2.7\text{ nM}$). Possibly, for the N^1 -acylated ureas **35–37**, the presence of the N^1 -carbonyl group may not form a new hydrogen bond within the enzyme catalytic site but increase the hydrophilicity instead, which is disadvantageous for the interaction with the lipophilic region in the enzyme near the tertiary pharmacophore binding site.

Moreover, the alkyl chain length between the secondary and tertiary pharmacophore was observed to play a subtle role in the sEH inhibitory activity. In general, the butyl linker was advantageous for the meta-substituted urea activity, whereas for the ortho- and para-substituted analogues, the inhibitory potency of propyl linked ureas was higher than that of the butyl ones. For example, the *p*-phenoxypropyl bridged compounds **16c** ($\text{IC}_{50} = 17.9\text{ nM}$) and **28c** ($\text{IC}_{50} = 3.3\text{ nM}$) displayed comparable potency to the *m*-phenoxybutyl bridged counterparts **17b** ($\text{IC}_{50} = 13.3\text{ nM}$) and **29b** ($\text{IC}_{50} = 2.7\text{ nM}$), respectively. However, for the potent N^4 -acetyl analogues, the activity difference between the butyl and propyl-linked ureas was slight (**28b** $\text{IC}_{50} = 3.6\text{ nM}$ vs **29b** $\text{IC}_{50} = 2.7\text{ nM}$).

The effect of the chain length to attach the piperazine pharmacophore was dependent on the N^4 -substitution, while the methylsulfonyl group as N^4 -substituent is favored for producing potent sEH inhibitors. Since the preliminary structure–activity relationship study indicated that the linker between the

Table 3. Inhibitory Activity against Human sEH and Melting Point of 1-Adamantan-1-yl-3-(3-(alkoxy)phenyl)urea Derivatives with Variation on the Carbon Chain Length between the Ether and Piperazine Pharmacophores and the N^4 -Substitution on the Piperazine Ring


Compd	R	n	Mp ^a (°C)	logP ^b	IC ₅₀ ^c (nM)	Compd	R	n	Mp ^a (°C)	logP ^b	IC ₅₀ ^c (nM)
23b		2	80~82	1.93	67.1	19b		2	78~80	3.04	2.8
24b	H	3	84~86	2.03	27.2	20b		3	150~153	3.14	2.9
25b		4	94~96	2.49	14.8	21b		4	135~137	3.60	7.1
26b		5	82~84	2.91	13.8	22b		5	72~74	4.01	11.7
15b	CH ₃	2	94~96	2.31	7.8	27b		2	73~75	1.58	6.0
16b		3	144~146	2.41	23.1	28b		3	96~98	1.68	3.6
17b		4	115~117	2.87	13.3	29b		4	76~78	2.14	2.7
18b		5	134~137	3.28	11.5	30b		5	136~138	2.55	2.8

^aMp, melting point. ^blog *P* (octanol/water partition coefficient) calculated by Crippen's method by using CS ChemDraw Ultra, version 9.0. ^cThe IC₅₀ values were determined by the fluorescent substrate-based assay on human sEH.³⁵

secondary ether and the tertiary piperazine pharmacophores as well as the N^4 -substitution on the piperazine was critical for the enzyme inhibition, the favored meta-substitution scaffold was selected as an effective platform to further compare the effect of the chain length and the N^4 -substitution on the potency. The enzyme IC₅₀ values of the ureas with variation on the alkyl chain length and the N^4 -piperazino substitution, and the calculated octanol–water partition coefficient (log *P*) of every molecule, are summarized in Table 3.

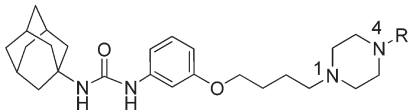
The linker length was examined from two to five methylene carbons with respect to the effect on the enzyme inhibition. As shown in Table 3, the effect was dependent on the N^4 -substitution of the piperazine pharmacophore. Basically, the polar piperazino functionality at this site was good for improving the physical properties as a “solubilizing” group, but the introduction of the carbonyl and the lipophilic group on N^4 -atom was beneficial for retaining the potency because of reduction of the polarity and the provision of a hydrogen bond acceptor. So an optimal balance between the polarity and the lipophilicity is favored to achieve excellent potency.

By analyzing the structure and the activity data in Table 3, we proposed the overall hydrophobicity (indicated by the octanol–water partition coefficient, i.e. log *P*) of the molecule and the presence of hydrogen bond acceptor structure as two major factors to determine the potency. For the N^4 -unsubstituted piperazine-containing ureas (compounds **23b–26b**), the enzyme inhibitory activity was highly correlated with the net hydrophobicity, while for the N^4 -carbonyl substituted piperazine-containing analogues (compounds **19b–22b**, **27b–30b**), the hydrophobicity and the hydrogen bond acceptor both contributed to the final enzyme IC₅₀ values. Especially for the N^4 -acetyl substituted piperazine series (compounds **27b–30b**), the resulting optimal log *P* and the presence of hydrogen bond acceptor conferred an attrac-

tive scaffold with low nanomolar IC₅₀ values against human sEH.

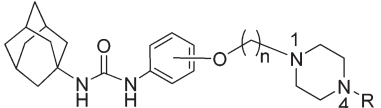
Apparently, the N^4 -substituent played an important role in the inhibitory potency of the ureas with piperazine as tertiary pharmacophore. So we selected the overall best inhibitor **29b** as the template to extend the structural diversity of the N^4 -substituent on piperazine. Because the acylation of the N^4 atom was beneficial for achieving high potency, we focused on the N^4 -acylation with different acyl groups and sulfonyl groups. As shown in Table 4, the sulfonyl substituted ureas (compounds **40** and **43**) were generally more potent than the acyl substituted analogues. The bulkier structure adjacent to the carbonyl or sulfonyl center was disfavored (**21b**, **41** vs **29b**, **43** vs **40**). The introduction of halogen into the acetyl group enhanced the interaction with the enzyme (**38** IC₅₀ = 1.8 nM; **39** IC₅₀ = 1.4 nM), possibly because of a new halogen bonding formation between the fluoro or chloro and the key residues in sEH.³⁹ The structural optimization on the N^4 -substitution afforded the most potent sEH inhibitor in the present work with improved physical properties (**40**, IC₅₀ = 1.0 nM, mp = 63–65 °C and *S* = 2.97 mg/mL), with the moderate melting points being low enough to make formulation easy but high enough that crystallization could be used for industrial production.

The bulky hydrophobic N^4 -substituent on piperazine tertiary pharmacophore helped improve the potency of the ortho-substituted ureas. We noticed that there were differences between the *tert*-butoxycarbonyl (Boc) and acetyl substituted ureas bearing a two to five methylene carbon chain linker with regard to the influence of the N^4 -substituent structure on the potency (Table 3). We were intrigued to incorporate the Boc and Ac group into N^4 -piperazine on the ortho-, meta-, and para-substituted phenyl linked ureas. Interestingly, a distinct enhancing effect was observed on

Table 4. Inhibition of Human sEH and Melting Point of 1-Adamantan-1-yl-3-(3-(4-(piperazin-1-yl)butoxy)phenyl)urea Derivatives with Variation on the N^4 -Substituent in Piperazine


Compd	R	Mp ^a (°C)	IC ₅₀ ^b (nM)
29b		76-78	2.7
21b		135-137	7.1
38		156-160	1.8
39		196-200	1.4
40		63-65	1.0
41		140-142	9.6
42		174-176	13.6
43		86-89	3.3

^aMp, melting point. ^bThe IC₅₀ values were determined by a recently developed sensitive fluorescence-based assay on human sEH.³⁵

Table 5. Inhibition of Human sEH and Their Change Fold of IC₅₀ Values of 1-Adamantan-1-ylurea Derivatives Possessing Piperazine Group in the Tertiary Pharmacophore Region, with N^4 -Acetyl and N^4 -Boc Substitution


substitution mode	compd	n	R	IC ₅₀ ^a (nM)	change fold ^b
ortho	28a	3	CH ₃ CO	990	25.2
	20a		^t BuOCO	39.4	
	29a	4	CH ₃ CO	3150	
	21a		^t BuOCO	16.5	
meta	28b	3	CH ₃ CO	3.6	1.2
	20b		^t BuOCO	2.9	
	29b	4	CH ₃ CO	2.7	
	21b		^t BuOCO	7.1	
para	28c	3	CH ₃ CO	3.3	-4.4
	20c		^t BuOCO	14.6	
	29c	4	CH ₃ CO	7.0	
	21c		^t BuOCO	20.1	

^aThe IC₅₀ values were determined by the sensitive fluorescence-based assay on human sEH.³⁵ ^bChange fold is the ratio of IC₅₀(R = CH₃CO)/IC₅₀(R = ^tBuOCO). The negative fold represents the ratio of IC₅₀(R = ^tBuOCO)/IC₅₀(R = CH₃CO).

the ortho-isomer from the para- and meta-isomers. As shown in Table 5, the replacement of a Ac group with Boc group on N^4 -piperazine of the ortho-substituted series resulted in a significant enhancement in the potency by a factor of 25- to 191-fold, affording nanomolar sEH inhibitors (**20a** IC₅₀ = 39.4 nM; **21a** IC₅₀ = 16.5 nM). However, for meta- or para-substituted analogues, the displacement of Ac by Boc on N^4 -atom suffered an activity decrease by a factor of 2- to 4-fold (**29b** IC₅₀ = 2.7 nM vs **21b** IC₅₀ = 7.1 nM; **28c** IC₅₀ = 3.3 nM vs **20c** IC₅₀ = 14.6 nM; **29c** IC₅₀ = 7.0 nM vs **21c** IC₅₀ = 20.1 nM).

Although it was not clear why the N^4 -Boc substituent significantly improved the potency of the ortho-substituted ureas, we speculated that the increasing hydrophobicity supplied by the *tert*-butyl carbamate group might be a major contribution factor. As a comparison, we synthesized an analogue containing an N^4 -methoxycarbonyl group (Figure 4). It was found that when the N^4 -piperazine was substituted by the small and relatively hydrophilic methyl carbamate, the enzyme inhibitory activity was sharply decreased by a factor of 231-fold (**44** IC₅₀ = 9100 nM) relative to the N^4 -*tert*-butoxycarbonyl analogue (**20a** IC₅₀ = 39.4 nM). As introduced above, the congestion of the neighboring ether and urea pharmacophores might lead to a poor potency of the ortho-substituted ureas. Correspondingly, the large hydrophobic group at N^4 -piperazine might compensate for the impaired interaction of the ortho-ureas with the enzyme. However, for the potent meta-substituted analogues (Figure 4B), the three acyl groups made a slight difference, ending up with almost equal potency (**20b** IC₅₀ = 2.9 nM; **28b** IC₅₀ = 3.6 nM; **45** IC₅₀ = 1.1 nM).

The ureas containing an N^4 -substituted piperazine as the tertiary pharmacophore were potent sEH inhibitors with improved physical and pharmacokinetic properties. The water solubility of some selected ureas was experimentally measured, and in vivo pharmacokinetic properties of six potent inhibitors (with IC₅₀ < 10 nM) were tested following oral administration in mice.³⁷ Encouragingly, the incorporation of N^4 -substituted piperazine into the urea-based sEH inhibitor as the tertiary pharmacophore conferred excellent water solubility and in vivo pharmacokinetic parameters with retention of potent enzyme inhibitory activity (Table 6).

As far as the structural effect on the solubility is concerned, the comparison of compounds **28a**, **28b**, and **28c** which just differed in the substitution pattern of the phenyl ring indicated that the ortho-substituted urea exhibited the best water solubility (**28a** *S* = 1.78 mg/mL). Meanwhile, among the meta-substituted ureas of **27b**, **28b**, and **29b** bearing different carbon chain length linkers, the four-methylene-carbon-linked urea displayed the highest water solubility (**29b** *S* = 1.82 mg/mL) which was also the most potent sEH inhibitor in this series. With respect to the influence of the N^4 -substituent on the solubility, meta-substituted ureas **16b**, **20b**, **24b**, and **28b** with variation on the N^4 -piperazine substitution pattern were tested and the N^4 -methyl-substituted one (**16b** *S* = 2.21 mg/mL) showed the highest water solubility. Finally, among all the tested compounds, the N^4 -sulfonyl substituted four-methylene-carbon linked urea (**40** *S* = 2.97 mg/mL) exhibited the highest water solubility.

We further investigated the pharmacokinetics of selected potent compounds (with IC₅₀ < 10 nM) in mice. As shown in Table 6, the in vivo pharmacokinetic parameters [time of maximum concentration (*T*_{max}), maximum concentration (*C*_{max}), half-life (*T*_{1/2}), and area under the curve (AUC)] of six compounds dissolved in a triglyceride of oleic oil (containing 3% EtOH) were determined following oral administration to mice at 5 mg/kg body weight.

The AUC is an expression of how much and how long a drug stays in the body, and it is related to the amount of drug absorbed systemically and the amount of drug metabolized, sequestered, and eliminated, while the *T*_{1/2} is more indicative of the rates of degradation, distribution, and elimination.⁴¹ Overall, the piperazine substituted ureas significantly improved the pharmacokinetics in comparison to the earlier inhibitor AUDA,⁴² in terms of the AUC and *T*_{1/2}. In the N^4 -Boc-piperazine ureas (**20b** and **21b**),

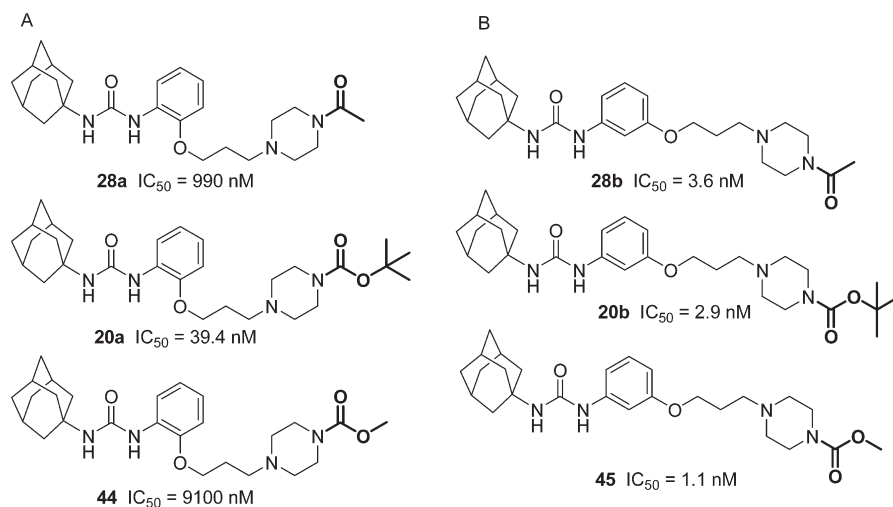


Figure 4. Structure and activity of the ortho- and meta-substituted ureas bearing different N^4 -substituents.

Table 6. Water Solubility of Some Selected Ureas with a Piperazine Present on the Tertiary Pharmacophore Region and the in Vivo Pharmacokinetic Parameters in Mice⁴⁰

compd	IC_{50}^a (nM)	S^b (mg/mL)	mp ($^{\circ}C$)	T_{max}^c (h)	C_{max}^d (nM)	$T_{1/2}^e$ (h)	AUC^f (nM·min)
16b	23.1	2.21	144–146				
20b	2.9	0.54	150–153	0.5	6	23	6000
21b	7.1	2.78	135–137	9	6	59	5100
24b	27.2	0.81	84–86				
27b	6.0	0.52	73–75				
28a	990	1.78	86–88				
28b	3.6	0.34	96–98	0.5	32	8	11100
28c	3.3	0.32	170–172	0.5	112	6	34800
29b	2.7	1.82	76–78				
29c	7.0	0.70	150–152	0.5	84	14	40200
40	1.0	2.97	63–65	0.5	160	3.5	20000
AUDA ^g	3	<0.125	142–143	1.3	14	2.1	3000

^aThe IC_{50} values were determined by the sensitive fluorescence-based assay on human sEH.³⁵ ^bExperimentally obtained solubility in sodium phosphate buffer (0.1 M, pH 7.4) at 25 ± 1.0 $^{\circ}C$.³⁴ ^c T_{max} , time of maximum concentration. ^d C_{max} , maximum concentration. ^e $T_{1/2}$, half-life. ^fAUC, area under the curve estimated from a plot of the inhibitor concentration in plasma (nM) versus time (minutes) following an oral dose of 5 mg/kg of the indicated compound given to mice in triglyceride ($N = 4$).⁴⁰ ^gThis compound was previously reported by Hammock's laboratory⁴¹ and used here as a reference.

relatively low AUC values were obtained while the half-lives were long, suggesting that the presence of an N^4 -Boc group might decrease the absorption. Interestingly, a significant increase in the C_{max} and AUC was observed with the compounds that carried a para-substituted phenyl ring (**28c** and **29c**) compared to the corresponding meta-substituted analogue (**28b**), indicating that the para-substituted pattern might be effective for producing excellent pharmacokinetic properties. Consistently, the most potent inhibitor **40** with a meta-substitution pattern exhibited high AUC value (AUC = 20 000 nM·min) but still less than the para-substituted analogues (**28c** AUC = 34 800 nM·min and **29c** AUC = 40 200 nM·min). However, the best compound, **40**, produced the highest C_{max} value ($C_{max} = 160$ nM) among the tested urea compounds. Furthermore, it is worthwhile noting that adamantane is often rapidly metabolized,^{43,44} however, in these more polar compounds containing the piperazine group as the tertiary pharmacophore, it does not appear to be as much a metabolic liability as in more lipophilic compounds.

Conclusion

This work focused on producing inhibitors of human sEH with improved physical and pharmacokinetic properties by

incorporating a piperazine functionality into the 1,3-disubstituted ureas as the tertiary pharmacophore. By investigation of the structural effect on the inhibition potency, physical properties (e.g., water solubility and melting point), and pharmacokinetic properties, a series of potent sEH inhibitors were identified with the meta- or para-substituted phenyl spacer, with N^4 -acetyl or sulfonyl substituted piperazine being the optimal structures. The corresponding N^4 -methanesulfonyl derivative (compound **40**) showed the lowest IC_{50} value and the best water solubility. There was an apparent trend that the bioavailability was closely related to the N^4 -substituent in piperazine, the substitution mode of phenyl spacer, and the carbon chain length between the secondary ether pharmacophore and piperazine. We demonstrated that 1-(4-(4-(4-acetylpiperazin-1-yl)butoxy)phenyl)-3-adamantan-1-ylurea (**29c**) and 1-(4-(3-(4-acetylpiperazin-1-yl)propoxy)phenyl)-3-adamantan-1-ylurea (**28c**) showed the best AUC, long half-life ($T_{1/2}$), and good maximum concentration (C_{max}) with a nanomolar IC_{50} value against human sEH enzyme. So the N^4 -substituted piperazine as the tertiary pharmacophore was significantly effective for improving the solubility and bioavailability of urea-based sEH inhibitors without any loss in potency. These findings are an important basis for the design and development of improved, orally available sEH inhibitors

as therapeutic agents for the treatment of hypertension and inflammation.

Experimental Section

¹H NMR spectra were recorded on a Varian Mercury 300 MHz spectrometer. The data are reported in parts per million relative to TMS and referenced to the solvent in which they were run. Signal multiplicities are represented as singlet (s), doublet (d), double doublet (dd), triplet (t), quartet (q), quintet (quint), multiplet (m), broad (br), and broad singlet (brs). Melting points (uncorrected) were determined on a Buchi-510 capillary apparatus. EI-MS spectra were obtained on a Finnigan MAT 95 mass spectrometer. ESI-MS spectra were obtained on a Finnigan LCQ Deca mass spectrometer. The purity of products was characterized by analytical HPLC and was more than 95% as determined by HPLC analyses with Vydac C18 column (4.6 mm × 250 mm) in two diverse systems and methods. System 1 consisted of the following: solvent A, 0.05% TFA in water; solvent B, 0.05% TFA in 95% acetonitrile. System 2 consisted of the following: solvent A, 0.05% TFA in water; solvent B, 0.05% TFA in methanol. Method A parameters were as follows: detection wavelength, 254 nm; flow rate, 2.0 mL/min; gradient, 10–90% of solvent B in 25 min. Method B parameters were as follows: detection wavelength, 254 nm; flow rate, 2.0 mL/min; gradient, 10–40% of solvent B in 2 min, then 40–90% of solvent B in 16 min. Method C parameters were as follows: detection wavelength, 225 nm; flow rate, 2.5 mL/min; gradient, 10–20% of solvent B in 2 min, then 20–60% of solvent B in 20 min, then 60–90% of solvent B in 2 min. Method D parameters were as follows: detection wavelength, 225 nm; flow rate, 2.5 mL/min; gradient, 10–20% of solvent B in 2 min, then 20–60% of solvent B in 16 min, then 60–90% of solvent B in 2 min.

The general procedures are exemplified by the preparation of compounds **16a**, **24a**, **28a**, **28b**, and **35** herein. The modified synthesis and the physical data for other target compounds are provided in Supporting Information.

1-Adamantan-1-yl-3-(2-(3-(4-methylpiperazin-1-yl)propoxy)phenyl)urea (16a). A solution of 1-methyl-4-(3-(2-nitrophenoxy)propyl)piperazine **8a** (200 mg, 0.72 mmol) in methanol was stirred under hydrogen overnight with palladium charcoal (10%, 20 mg) as a catalyst. After filtration and removal of the solvent, 2-(3-(4-methylpiperazin-1-yl)propoxy)aniline was obtained as an unstable brown solid (174 mg, 97% yield). The aniline was used in the next step without further purification. A solution of 1-isocyanatoadamantane (85 mg, 0.48 mmol) in dry CH₂Cl₂ (10 mL) was added to 2-(3-(4-methylpiperazin-1-yl)propoxy)aniline (100 mg, 0.40 mmol) in dry CH₂Cl₂ (10 mL). The mixture was stirred at room temperature overnight. The solvent was removed at reduced pressure and the residue was purified by silica gel chromatography (CH₂Cl₂/CH₃OH = 10:1) to afford **16a** as a white powder (134 mg, 79% yield). ¹H NMR (300 MHz, CDCl₃) δ 1.69 (s, 6H), 2.07–2.09 (m, 11H), 2.31 (s, 3H), 2.53–2.61 (m, 10H), 4.05 (t, 2H, *J* = 6.3 Hz), 4.73 (brs, 1H), 6.78–6.85 (m, 2H), 6.88–6.93 (m, 2H), 8.01–8.05 (m, 1H); ESI-MS *m/z* calcd for C₂₅H₃₉N₄O₂ [M + H]⁺, 427.6; found [M + H]⁺, 427.3; mp 154–156 °C. Purity: system 1, 97.8% (method C, *t_R* = 19.92 min); system 2, 100% (method D, *t_R* = 23.48 min).

1-Adamantan-1-yl-3-(2-(3-(piperazin-1-yl)propoxy)phenyl)urea (24a). To a stirred solution of *tert*-butyl 4-(3-(2-(3-(adamantan-1-yl)ureido)phenoxy)propyl)piperazine-1-carboxylate **20a** (101 mg, 0.2 mmol) in CH₂Cl₂ (6 mL) was added 0.3 mL of CF₃COOH at 0 °C. The solution was stirred at 0 °C overnight and then was evaporated to dryness in vacuum. The residue was dissolved in water (10 mL) and then basified with 5% NaOH and extracted with CH₂Cl₂. The organic layer was washed with brine and dried over Na₂SO₄. Evaporation in vacuum gave 1-adamantan-1-yl-3-(2-(3-(piperazin-1-yl)propoxy)phenyl)urea **24a** (70 mg, 86% yield) as a white powder. ¹H NMR (300 MHz, CDCl₃) δ 1.69 (s, 6H), 2.04 (s, 6H), 2.08–2.17 (m, 3H), 2.57–2.65 (m, 6H), 2.98

(t, 4H), 4.05 (t, 2H), 5.29 (brs, 1H), 6.80–6.83 (m, 1H), 6.89–6.92 (m, 3H), 8.04–8.07 (m, 1H); EI-MS *m/z* calcd for C₂₄H₃₆N₄O₂ [M]⁺, 412; found [M]⁺, 412; mp 162–164 °C. Purity: system 1, 98.6% (method A, *t_R* = 17.89 min); system 2, 96.9% (method B, *t_R* = 25.43 min).

1-Adamantan-1-yl-3-(2-(3-(4-acetyl-piperazin-1-yl)propoxy)phenyl)urea (28a). A solution of acetic anhydride (13 mg, 0.13 mmol) and 1-adamantan-1-yl-3-(2-(3-(piperazin-1-yl)propoxy)phenyl)urea **24a** (43 mg, 0.10 mmol) in DMF (8 mL) was stirred for 10 h at room temperature. Then the solvent was evaporated. The residue was partitioned between ether (30 mL) and water (30 mL). The ether layer was dried over Na₂SO₄ and evaporated. The residue was purified by column chromatography on silica gel, eluting with (CH₂Cl₂/CH₃OH = 10:1) to yield 21 mg (44%) of **28a** as a white powder. ¹H NMR (300 MHz, CDCl₃) δ 1.69 (s, 6H), 2.04–2.11 (m, 14H), 2.75 (m, 4H), 2.87 (t, 2H, *J* = 7.8 Hz), 3.63 (t, 2H, *J* = 5.1 Hz), 3.99 (t, 2H, *J* = 5.4 Hz), 6.22 (s, 1H), 6.72–6.75 (m, 1H), 6.82–6.93 (m, 2H), 7.37 (s, 1H), 8.23–8.26 (m, 1H); EI-MS *m/z* calcd for C₂₆H₃₈N₄O₃ [M]⁺, 454; found [M]⁺, 454; mp 86–88 °C. Purity: system 1, 100% (method A, *t_R* = 20.13 min); system 2, 100% (method B, *t_R* = 24.95 min).

1-Adamantan-1-yl-3-(3-(3-(4-acetyl-piperazin-1-yl)propoxy)phenyl)urea (28b). 1-(4-(3-(3-nitrophenoxy)propyl)piperazin-1-yl)ethanone **12e** (54 mg, 0.18 mmol) dissolved in methanol was stirred in an atmosphere of hydrogen overnight with palladium charcoal (10%, 6 mg) as a catalyst. After filtration and removal of the solvent, 1-(4-(3-(3-aminophenoxy)propyl)piperazin-1-yl)ethanone was obtained as a yellow oil (42 mg, 86% yield). ¹H NMR (300 MHz, CDCl₃) δ 1.95–1.98 (m, 2H), 2.09 (s, 3H), 2.43–2.50 (m, 4H), 2.53–2.58 (m, 2H), 3.49 (t, 2H, *J* = 4.2 Hz), 3.65 (t, 2H, *J* = 4.8 Hz), 3.99 (t, 2H, *J* = 6.3 Hz), 6.23–6.24 (m, 1H), 6.27–6.33 (m, 2H), 7.04 (t, 1H, *J* = 7.8 Hz). A solution of 1-isocyanatoadamantane (29 mg, 0.17 mmol) in dry CH₂Cl₂ (5 mL) was added to 1-(4-(3-(3-aminophenoxy)propyl)piperazin-1-yl)ethanone (42 mg, 0.15 mmol) in dry CH₂Cl₂ (10 mL) at 0 °C. The mixture was stirred at room temperature overnight. The solvent was removed at reduced pressure and the residue was purified by silica gel chromatography (CH₂Cl₂/CH₃OH = 10:1) to afford **28b** as a white powder (39 mg, 57% yield). ¹H NMR (300 MHz, CDCl₃) δ 1.68 (s, 6H), 1.95–2.01 (m, 8H), 2.09 (m, 6H), 2.45–2.59 (m, 6H), 3.50 (t, 2H, *J* = 4.5 Hz), 3.64–3.67 (m, 2H), 4.01 (t, 2H, *J* = 6.0 Hz), 4.51 (s, 1H), 6.12 (s, 1H), 6.57 (dd, 1H, *J* = 2.7 Hz, *J* = 5.1 Hz), 6.72 (d, 1H, *J* = 8.1 Hz), 7.15 (t, 1H, *J* = 8.4 Hz); EI-MS *m/z* calcd for C₂₆H₃₈N₄O₃ [M]⁺, 454; found [M]⁺, 454; mp 96–98 °C. Purity: system 1, 98.7% (method A, *t_R* = 19.93 min); system 2, 100% (method B, *t_R* = 25.18 min).

***tert*-Butyl 4-(4-(3-(3-nitrophenoxy)butanoyl)piperazine-1-carboxylate (33)**. A solution of compound **32** (148 mg, 0.66 mmol), EDCI (127 mg, 0.66 mmol), and HOAt (90 mg, 0.66 mmol) in dry CH₂Cl₂ was stirred at 0 °C for 30 min. To this solution was added *tert*-butyl piperazine-1-carboxylate (135 mg, 0.72 mmol). The reaction mixture was allowed to warm to room temperature, and DIPEA (0.13 mL) was added. The solution was stirred for 5 h and then extracted with dichloromethane. The combined organic layers were washed with saturated NaHCO₃ aqueous solution and brine and dried over Na₂SO₄. The concentration provided the residue which was purified by chromatography using CH₂Cl₂/CH₃OH (10:1) as eluent to give compound **33** (237 mg, 91%) as a white solid. ¹H NMR (300 MHz, CDCl₃) δ 1.47 (s, 9H), 2.19 (t, 2H, *J* = 6.6 Hz), 2.55 (t, 2H, *J* = 7.2 Hz), 3.40–3.45 (m, 6H), 3.61 (t, 2H, *J* = 4.5 Hz), 4.12 (t, 2H, *J* = 6.0 Hz), 7.20–7.24 (m, 1H), 7.42 (t, 1H, *J* = 8.1 Hz), 7.23 (t, 1H, *J* = 2.1 Hz), 7.79–7.83 (m, 1H).

***tert*-Butyl 4-(4-(3-(3-aminophenoxy)butanoyl)piperazine-1-carboxylate (34)**. *tert*-Butyl 4-(4-(3-nitrophenoxy)butanoyl)piperazine-1-carboxylate **33** (98 mg, 0.25 mmol) dissolved in methanol was stirred in an atmosphere of hydrogen overnight with palladium charcoal (10%, 10 mg) as a catalyst. After filtration and removal of the solvent, *tert*-butyl 4-(4-(3-aminophenoxy)butanoyl)piperazine-1-carboxylate **33** was obtained as a

white solid (174 mg, 97% yield) which was used in next step without further purification.

tert-Butyl 4-(4-(3-(3-Adamantan-1-ylureido)phenoxy)butanoyl)-piperazine-1-carboxylate (35). A solution of 1-isocyanatoadamantane (49 mg, 0.275 mmol) in dry CH_2Cl_2 was added dropwise to a solution of **34** (0.25 mmol) in dry CH_2Cl_2 at 0 °C. The mixture was stirred at room temperature overnight. The solvent was removed at reduced pressure and the residue was purified by silica gel chromatography ($\text{CH}_2\text{Cl}_2/\text{CH}_3\text{OH} = 30:1$) to afford **35** as a pale brown powder (118 mg, 87% yield). ^1H NMR (300 MHz, CDCl_3) δ 1.47 (s, 9H), 1.68 (s, 6H), 2.08 (s, 6H), 2.10–2.13 (m, 5H), 2.52 (t, 2H, $J = 7.5$ Hz), 3.40–3.44 (m, 6H), 3.58–3.61 (m, 2H), 3.99 (t, 2H, $J = 5.7$ Hz), 4.63 (s, 1H), 6.32 (s, 1H), 6.55 (dd, 1H, $J = 8.1$ Hz, $J = 2.1$ Hz), 6.75 (dd, 1H, $J = 8.1$ Hz, $J = 1.2$ Hz), 6.99 (s, 1H), 7.14 (t, 1H, $J = 7.8$ Hz); EI-MS m/z calcd for $\text{C}_{30}\text{H}_{44}\text{N}_4\text{O}_5$ $[\text{M}]^+$, 540; found $[\text{M}]^+$, 540; mp 100–104 °C. Purity: system 1, 99.7% (method A, $t_{\text{R}} = 32.20$ min); system 2, 100% (method B, $t_{\text{R}} = 33.14$ min).

Solubility. Water solubility was determined experimentally in sodium phosphate buffer (0.1 M, pH 7.4) as previously described at 25 ± 1.5 °C.³⁴

Enzyme Preparation. Recombinant human sEH was produced in a polyhedron positive baculovirus expression system following cloning and sequencing in this laboratory and was purified by affinity chromatography as previously reported.^{45,46}

IC₅₀ Assay Conditions. IC₅₀ values were determined as described using a sensitive fluorescent-based assay,³⁵ and a brief description of the procedure is as follows: cyano(2-methoxy-naphthalen-6-yl)methyl *trans*-(3-phenyloxyran-2-yl) methyl carbonate (CMNPC) was used as a fluorescent substrate. Human sEH (1 nM) was incubated with inhibitors for 5 min in pH 7.0 Bis-Tris/HCl buffer (25 mM) containing 0.1 mg/mL BSA at 30 °C prior to substrate introduction ($[\text{S}] = 5 \mu\text{M}$). Activity was measured by determining the appearance of the 6-methoxy-2-naphthaldehyde with an excitation wavelength of 330 nm and an emission wavelength of 465 nm for 10 min. IC₅₀ results are averages of three replicates. The fluorescent assay as performed here has a standard error between 10% and 20%, suggesting that differences of 2-fold or greater are significant.

In Vivo Pharmacokinetic Studies. In vivo experiments were performed following protocols approved by the U.C.D. Animal Use and Care Committee. Mice were treated with test compounds orally at 5 mg/kg. Compounds were given by oral gavage in 0.1 mL of oleic oil solution containing 3% EtOH. Then 10 μL of blood was collected from mice tail vein before drug administration and 30, 60, 90, 120, 240, 450, 600, and 1440 min after drug administration ($N = 3$). The samples were centrifuged at 3000 rpm at 4 °C for 10 min, and the plasma samples were collected for instrumental analysis. Blood sample preparation and LC/MS/MS analyses were performed as previously reported.⁴⁰ Pharmacokinetic parameters (AUC and $T_{1/2}$) were calculated by fitting the blood concentration–time data to a noncompartmental model with WinNonlin 5.0 (Pharsight, CA). Data are average results obtained from at least three different animals.

Acknowledgment. The work in Y.-Q.L.'s lab was supported by National Science and Technology Major Project "Key New Drug Creation and Manufacturing Program", China (Grants 2009ZX09301-001 and 2009ZX09103-067). Partial support was obtained from NIEHS Grant R01 ES002710 and NIH/NHLBI Grant R01 HL059699. B.D.H. is a George and Judy Marcus Senior Fellow of the American Asthma Foundation.

Supporting Information Available: Details of the synthetic procedures; physical data for compounds **15b**, **16b–c**, **17a–c**, **18b**, **19b**, **20a–c**, **21a–c**, **22b**, **23b**, **24b–c**, **25a–c**, **26b**, **27b**, **28c**, **29a–c**, **30b**, **36–45**. This material is available free of charge via the Internet at <http://pubs.acs.org>.

References

- Hammock, B. D.; Grant, D.; Storms, D. Epoxide Hydrolase. In *Comprehensive Toxicology*; Sipes, I., McQueen, C., Gandolfi, A., Eds.; Pergamon: Oxford, U.K., 1997; pp 283–305.
- Levin, W.; Michaud, D. P.; Thomas, P. E.; Jerina, D. M. Distinct rat hepatic microsomal epoxide hydrolases catalyze the hydration of cholesterol 5,6- α -oxide and certain xenobiotic alkene and arene oxides. *Arch. Biochem. Biophys.* **1983**, *220*, 485–494.
- Pace-Asciak, C. R.; Lee, W. S. Purification of hepxoxilin epoxide hydrolase from rat liver. *J. Biol. Chem.* **1989**, *264*, 9310–9313.
- Morisseau, C.; Hammock, B. D. Epoxide hydrolases: mechanisms, inhibitor designs, and biological roles. *Annu. Rev. Pharmacol. Toxicol.* **2005**, *45*, 311–333.
- Imig, J. D.; Hammock, B. D. Soluble epoxide hydrolase as a therapeutic target for cardiovascular diseases. *Nat. Rev. Drug Discovery* **2009**, *8*, 794–805.
- (a) Capdevila, J. H.; Falck, J. R.; Harris, R. C. Cytochrome P450 and arachidonic acid bioactivation: molecular and functional properties of the arachidonate monooxygenase. *J. Lipid Res.* **2000**, *41*, 163–181. (b) Fretland, A. J.; Omiecinski, C. J. Epoxide hydrolases: biochemistry and molecular biology. *Chem.-Biol. Interact.* **2000**, *129*, 41–59. (c) Meijer, J.; Depierre, J. W. Cytosolic epoxide hydrolase. *Chem.-Biol. Interact.* **1988**, *64*, 207–249.
- Zeldin, D. C. Epoxygenase pathways of arachidonic acid metabolism. *J. Biol. Chem.* **2001**, *276*, 36059–36062.
- (a) Watanabe, H.; Vriens, J.; Prenen, J.; Droogmans, G.; Voets, T.; Nilius, B. Anandamide and arachidonic acid use epoxyeicosatrienoic acids to activate TRPV4 channels. *Nature* **2003**, *424*, 434–438. (b) Earley, S.; Heppner, T. J.; Nelson, M. T.; Brayden, J. E. TRPV4 forms a novel Ca^{2+} signaling complex with ryanodine receptors and BKCa channels. *Circ. Res.* **2005**, *97*, 1270–1279. (c) Vriens, J.; Owsianik, G.; Fisslthaler, B.; Suzuki, M.; Janssens, A.; Voets, T.; Morisseau, C.; Hammock, B. D.; Fleming, I.; Busse, R.; Nilius, B. Modulation of the Ca^{2+} permeable cation channel TRPV4 by cytochrome P450 epoxygenases in vascular endothelium. *Circ. Res.* **2005**, *97*, 908–915.
- Larsen, B. T.; Campbell, W. B.; Guttermann, D. B. Beyond vasodilation: nonvasomotor roles of epoxyeicosatrienoic acids in the cardiovascular system. *Trends Pharmacol. Sci.* **2007**, *28*, 32–38.
- Yang, B.; Graham, L.; Dikalov, S.; Mason, R. P.; Falck, J. R.; Liao, J. K.; Zeldin, D. C. Overexpression of cytochrome P450 CYP2J2 protects against hypoxia-reoxygenation injury in cultured bovine aortic endothelial cells. *Mol. Pharmacol.* **2001**, *60*, 310–320.
- Sun, J.; Sui, X.; Bradbury, J. A.; Zeldin, D. C.; Conte, M. S.; Liao, J. K. Inhibition of vascular smooth muscle cell migration by cytochrome P450 epoxygenase-derived eicosanoids. *Circ. Res.* **2002**, *90*, 1020–1027.
- Node, K.; Ruan, X.; Dai, J.; Yang, S.; Graham, L.; Zeldin, D. C.; Liao, J. K. Activation of $\text{G}_{\alpha\text{q}}$ mediates induction of tissue-type plasminogen activator gene transcription by epoxyeicosatrienoic acids. *J. Biol. Chem.* **2001**, *276*, 15983–15989.
- Spector, A. A.; Fang, X.; Snyder, G. D.; Weintraub, N. L. Epoxyeicosatrienoic acids (EETs): metabolism and biochemical function. *Prog. Lipid Res.* **2004**, *43*, 55–90.
- Marino, J. P., Jr. Soluble epoxide hydrolase, a target with multiple opportunities for cardiovascular drug discovery. *Curr. Top. Med. Chem.* **2009**, *9*, 452–463.
- Yu, Z.; Xu, F.; Huse, L. M.; Morisseau, C.; Draper, A. J.; Newman, J. W.; Parker, C.; Graham, L.; Engler, M. M.; Hammock, B. D.; Zeldin, D. C.; Kroetz, D. L. Soluble epoxide hydrolase regulates hydrolysis of vasoactive epoxyeicosatrienoic acids. *Circ. Res.* **2000**, *87*, 992–998.
- Imig, J. D.; Zhao, X.; Capdevila, J. H.; Morisseau, C.; Hammock, B. D. Soluble epoxide hydrolase inhibition lowers arterial blood pressure in angiotensin II hypertension. *Hypertension* **2002**, *39*, 690–694.
- Zhao, X.; Yamamoto, T.; Newman, J. W.; Kim, I.-H.; Watanabe, T.; Hammock, B. D.; Stewart, J.; Pollock, J. S.; Pollock, D. M.; Imig, J. D. Soluble epoxide hydrolase inhibition protects the kidney from hypertension-induced damage. *J. Am. Soc. Nephrol.* **2004**, *15*, 1244–1253.
- Imig, J. D.; Zhao, X.; Zaharis, C. Z.; Olearczyk, J. J.; Pollock, D. M.; Newman, J. W.; Kim, I.-H.; Watanabe, T.; Hammock, B. D. An orally active epoxide hydrolase inhibitor lowers blood pressure and provides renal protection in salt-sensitive hypertension. *Hypertension* **2005**, *46*, 975–981.
- Arete Therapeutics initiates a phase IIa clinical trial for AR9281, a novel sEH inhibitor to treat type 2 diabetes. See additional information on <http://www.fiarebiotech.com/tags/arete-therapeutics>.
- Hwang, S. H.; Tsai, H.-J.; Liu, J.-Y.; Morisseau, C.; Hammock, B. D. Orally bioavailable potent soluble epoxide hydrolase inhibitors. *J. Med. Chem.* **2007**, *50*, 3825–3840.

- (21) Xie, Y. L.; Liu, Y. D.; Gong, G. L.; Smith, D. H.; Yan, F.; Rinderspacher, A.; Feng, Y.; Zhu, Z. X.; Li, X. P.; Deng, S. X.; Branden, L.; Vidovic, D.; Chung, C.; Schurer, S.; Morisseau, C.; Hammock, B. D.; Landry, D. W. Discovery of potent non-urea inhibitors of soluble epoxide hydrolase. *Bioorg. Med. Chem. Lett.* **2009**, *19*, 2354–2359.
- (22) Eldrup, A. B.; Soleymanzadeh, F.; Taylor, S. J.; Muegge, I.; Farrow, N. A.; Joseph, D.; McKellop, K.; Man, C. C.; Kukulka, A.; De Lombaert, S. Structure-based optimization of arylamides as inhibitors of soluble epoxide hydrolase. *J. Med. Chem.* **2009**, *52*, 5880–5895.
- (23) Anandan, S. K.; Webb, H. K.; Do, Z. N.; Gless, R. D. Unsymmetrical non-adamantyl *N,N'*-diaryl urea and amide inhibitors of soluble epoxide hydrolase. *Bioorg. Med. Chem. Lett.* **2009**, *19*, 4259–4263.
- (24) Shen, H. C.; Ding, F. X.; Deng, Q.; Xu, S.; Chen, H. S.; Tong, X.; Tong, V.; Zhang, X.; Chen, Y.; Zhou, G.; Pai, L. Y.; Alonso-Galicia, M.; Zhang, B.; Roy, S.; Tata, J. R.; Berger, J. P.; Colletti, S. L. Discovery of 3,3-disubstituted piperidine-derived trisubstituted ureas as highly potent soluble epoxide hydrolase inhibitors. *Bioorg. Med. Chem. Lett.* **2009**, *19*, 5314–5320.
- (25) Shen, H. C.; Ding, F. X.; Wang, S.; Deng, Q.; Zhang, X.; Chen, Y.; Zhou, G.; Xu, S.; Chen, H. S.; Tong, X.; Tong, V.; Mitra, K.; Kumar, S.; Tsai, C.; Stevenson, A. S.; Pai, L. Y.; Alonso-Galicia, M.; Chen, X.; Soisson, S. M.; Roy, S.; Zhang, B.; Tata, J. R.; Berger, J. P.; Colletti, S. L. Discovery of a highly potent, selective, and bioavailable soluble epoxide hydrolase inhibitor with excellent ex vivo target engagement. *J. Med. Chem.* **2009**, *52*, 5009–5012.
- (26) Kowalski, J. A.; Swinamer, A. D.; Muegge, I.; Eldrup, A. B.; Kukulka, A.; Cywin, C. L.; De Lombaert, S. Rapid synthesis of an array of trisubstituted urea-based soluble epoxide hydrolase inhibitors facilitated by a novel solid-phase method. *Bioorg. Med. Chem. Lett.* **2010**, *20*, 3703–3707.
- (27) Eldrup, A. B.; Soleymanzadeh, F.; Farrow, N. A.; Kukulka, A.; De Lombaert, S. Optimization of piperidyl-ureas as inhibitors of soluble epoxide hydrolase. *Bioorg. Med. Chem. Lett.* **2010**, *20*, 571–575.
- (28) Kim, I. -H.; Morisseau, C.; Watanabe, T.; Hammock, B. D. Design, synthesis, and biological activity of 1,3-disubstituted ureas as potent inhibitors of the soluble epoxide hydrolase of increased water solubility. *J. Med. Chem.* **2004**, *47*, 2110–2122.
- (29) Kim, I. H.; Heirtzler, F. R.; Morisseau, C.; Nishi, K.; Tsai, H.-J.; Hammock, B. D. Optimization of amide-based inhibitors of soluble epoxide hydrolase with improved water solubility. *J. Med. Chem.* **2005**, *48*, 3621–3629.
- (30) Kim, I. H.; Nishi, K.; Tsai, H. J.; Bradford, T.; Koda, Y.; Watanabe, T.; Morisseau, C.; Blanchfield, J.; Toth, I.; Hammock, B. D. Design of bioavailable derivatives of 12-(3-adamantan-1-yl-ureido)dodecanoic acid, a potent inhibitor of the soluble epoxide hydrolase. *Bioorg. Med. Chem.* **2007**, *15*, 312–323.
- (31) Watanabe, T.; Schulz, D.; Morisseau, C.; Hammock, B. D. High-throughput pharmacokinetic method: cassette dosing in mice associated with minuscule serial bleedings and LC/MS/MS analysis. *Anal. Chim. Acta* **2006**, *559*, 37–44.
- (32) Todorovic, A.; Haskell-Luevano, C. A review of melanocortin receptor small molecule ligands. *Peptides* **2005**, *26*, 2026–2036.
- (33) Kundu, B. Solid-phase strategies for the design and synthesis of heterocyclic molecules of medicinal interest. *Curr. Opin. Drug Discovery Dev.* **2003**, *6*, 815–826.
- (34) Li, H. Y.; Jin, Y.; Morisseau, C.; Hammock, B. D.; Long, Y. Q. The 5-substituted piperazine as a novel secondary pharmacophore greatly improving the physical properties of urea-based inhibitors of soluble epoxide hydrolase. *Bioorg. Med. Chem.* **2006**, *14*, 6586–6592.
- (35) Jones, P. D.; Wolf, N. M.; Morisseau, C.; Whetstone, P.; Hock, B.; Hammock, B. D. Fluorescent substrates for soluble epoxide hydrolase and application to inhibition studies. *Anal. Biochem.* **2005**, *343*, 66–75.
- (36) Jones, P. D.; Tsai, H.-J.; Do, Z. N.; Morisseau, C.; Hammock, B. D. Synthesis and SAR of conformationally restricted inhibitors of soluble epoxide hydrolase. *Bioorg. Med. Chem. Lett.* **2006**, *16*, 5212–5216.
- (37) Anandan, S.-K.; Gless, R. D. Exploration of secondary and tertiary pharmacophores in unsymmetrical *N,N'*-diaryl urea inhibitors of soluble epoxide hydrolase. *Bioorg. Med. Chem. Lett.* **2010**, *20*, 2740–2744.
- (38) Argiriadi, M. A.; Morisseau, C.; Hammock, B. D.; Christianson, D. W. Detoxification of environmental mutagens and carcinogens: structure, mechanism, and evolution of liver epoxide hydrolase. *Proc. Natl. Acad. Sci. U.S.A.* **1999**, *96*, 10637–10642.
- (39) Lu, Y. X.; Shi, T.; Wang, Y.; Yang, H. Y.; Yan, X. H.; Luo, X. M.; Jiang, H. L.; Zhu, W. L. Halogen bonding—a novel interaction for rational drug design? *J. Med. Chem.* **2009**, *52*, 2854–2862.
- (40) Liu, J. Y.; Tsai, H. J.; Hwang, S. H.; Jones, P. D.; Morisseau, C.; Hammock, B. D. Pharmacokinetic optimization of four soluble epoxide hydrolase inhibitors for use in a murine model of inflammation. *Br. J. Pharmacol.* **2009**, *156*, 284–296.
- (41) Kim, I. -H.; Tsai, H. -J.; Nishi, K.; Kasagami, T.; Morisseau, C.; Hammock, B. D. 1,3-Disubstituted ureas functionalized with ether groups are potent inhibitors of the soluble epoxide hydrolase with improved pharmacokinetic properties. *J. Med. Chem.* **2007**, *50*, 5217–5226.
- (42) Morisseau, C.; Goodrow, M. H.; Newman, J. W.; Wheelock, C. E.; Dowdy, D. L.; Hammock, B. D. Structural refinement of inhibitors of urea-based soluble epoxide hydrolases. *Biochem. Pharmacol.* **2002**, *63*, 1599–1608.
- (43) Tsai, H.-J.; Hwang, S. H.; Morisseau, C.; Yang, J.; Jones, P. D.; Kasagami, T.; Kim, I.-H.; Hammock, B. D. Pharmacokinetic screening of soluble epoxide hydrolase inhibitors in dogs. *Eur. J. Pharm. Sci.* **2010**, *40*, 222–238.
- (44) Ulu, A.; Davis, B. B.; Tsai, H.-J.; Kim, I.-H.; Morisseau, C.; Inceoglu, B.; Fiehn, O.; Hammock, B. D.; Weiss, R. H. Soluble epoxide hydrolase inhibitors reduce the development of atherosclerosis in apolipoprotein E-knockout mouse model. *J. Cardiovasc. Pharmacol.* **2008**, *52*, 314–323.
- (45) Beetham, J. K.; Tian, T.; Hammock, B. D. cDNA cloning and expression of a soluble epoxide hydrolase from human liver. *Arch. Biochem. Biophys.* **1993**, *305*, 197–201.
- (46) Wixtrom, R. N.; Silva, M. H.; Hammock, B. D. Affinity purification of cytosolic epoxide hydrolase using derivatized epoxy-activated sepharose gels. *Anal. Biochem.* **1988**, *169*, 71–80.